Pellino-2 in nonimmune cells: novel interaction partners and intracellular localization

Ileana Cristea[1] (iD), Ove Bruland[2] (iD), Ingvild Aukrust[2,3] (iD), Eyvind Rødahl[1,4] (iD) and Cecilie Bredrup[1,4] (iD)

1 Department of Clinical Medicine, University of Bergen, Norway
2 Department of Medical Genetics, Haukeland University Hospital, Bergen, Norway
3 Department of Clinical Science, University of Bergen, Norway
4 Department of Ophthalmology, Haukeland University Hospital, Bergen, Norway

Pellino-2 is an E3 ubiquitin ligase that mediates intracellular signaling in innate immune pathways. Most studies of endogenous Pellino-2 have been performed in macrophages, but none in nonimmune cells. Using yeast two-hybrid screening and co-immunoprecipitation, we identified six novel interaction partners of Pellino-2, with various localizations: insulin receptor substrate 1, NIMA-related kinase 9, tumor necrosis factor receptor-associated factor 7, cyclin-F, roundabout homolog 1, and disheveled homolog 2. Pellino-2 showed cytoplasmic localization in a wide range of nonimmune cells under physiological potassium concentrations. Treatment with the potassium ionophore nigericin resulted in nuclear localization of Pellino-2, which was reversed by the potassium channel blocker tetraethylammonium. Live-cell imaging revealed intracellular migration of GFP-tagged Pellino-2. In summary, Pellino-2 interacts with proteins at different cellular locations, taking part in dynamic processes that change its intracellular localization influenced by potassium efflux.

Keywords: CYCLIN-F; DVL-2; IRS-1; NEK9; ROBO-1; TRAF7

The Pellino protein was initially identified in *Drosophila* as a binding partner of Pelle [the *Drosophila* homologue of interleukin-1 receptor-associated kinase (IRAK) proteins] [1]. In mammals, the Pellino proteins constitute a family of four E3 ubiquitin ligases: Pellino-1, Pellino-2, and two isoforms of Pellino-3 (Pellino-3a and -3b). They modulate Toll-like receptor (TLR) signaling via multiple mechanisms [2,3]. Pellino-1 facilitates TLR3 and TLR4 activation, leading to proinflammatory cytokine production [4], while Pellino-3 downregulates TLR3-induced expression of type I interferons [5]. Pellino-3 also downregulates interleukin 1β (IL-1β) expression, protecting against obesity-induced inflammation and insulin resistance [6]. Pellino-2 facilitates lipopolysaccharide-induced activation of extracellular signal-regulated kinase (ERK) and c-Jun N-terminal kinase (JNK) mitogen-activated protein kinase (MAPK) pathways [7], leading to NACHT, LRR, and PYD domains-containing protein 3 (NLRP3) inflammasome activation and production of IL-1β [8,9].

Abbreviations

ASC, apoptosis-associated speck-like protein; ATPIF1, ATPase inhibitory factor 1; DVL-2, disheveled homolog 2; eGFP, enhanced GFP; HEK293, human embryonic kidney cells 293; IgG, immunoglobulin G; IL-1β, interleukin 1β; IRAK-1/4, interleukin-1 receptor-associated kinase 1/4; IRS-1, insulin receptor substrate 1; K+, potassium ions; LAMP-1, lysosomal-associated membrane protein 1; LNCaP, lymph node carcinoma of the prostate cell line; NEK9, NIMA-related kinase 9; NLRP3, NACHT, LRR, and PYD domains-containing protein 3; PB, phosphate buffer; PEST, peptide sequence rich in proline, glutamic acid, serine, and threonine; PFA, paraformaldehyde; PML, promyelocytic leukemia bodies; RING, really interesting new gene domain; ROBO-1, roundabout homolog 1; TAK-1, transforming growth factor β (TGFβ)-activated kinase 1; TEA, tetraethylammonium; TLR, Toll-like receptor; TRAF6/7, tumor necrosis factor (TNF) receptor-associated factor 6/7.

Structurally, Pellino-2 consists of an N-terminal forkhead-associated (FHA) domain that binds to phospho-threonine epitopes on target proteins [10], and a C-terminal really interesting new gene domain (RING)-like domain that catalyzes the poly-ubiquitination of substrates. This RING-like domain is a characteristic feature of many E3 ubiquitin ligases [11]. Pellino-2 associates with several signaling proteins involved in the TLR pathways, including IL-1 receptor-associated kinases IRAK-1 [10–15] and IRAK-4 [13,16], transforming growth factor β (TGFβ)-activated kinase 1 (TAK-1; 14, 17) and tumor necrosis factor (TNF) receptor-associated factor 6 (TRAF6; 14, 15, 17). Pellino-2 has been shown to promote Lys-63-mediated polyubiquitination of IRAK-1 and IRAK-4, while at the same time being a phosphorylation substrate for the same proteins [13,16]. In co-immunoprecipitation experiments, Pellino-2 was shown to bind to both TRAF6 and TAK-1 [13,16].

Pellino-2 has been studied mainly in macrophages, and we recently showed that Pellino-2 co-localizes with NLRP3 and apoptosis-associated speck-like protein (ASC) during inflammasome activation in macrophages. Furthermore, we observed a relocation of Pellino-2 upon inflammasome activation that was influenced by potassium (K^+) efflux [9]. Depletion of intracellular K^+ has been shown to be the necessary and sufficient cellular event to activate the NLRP3 inflammasome [17].

Given that little is known about Pellino-2 in nonimmune cells, we examined Pellino-2 in a variety of non-immune cells. We found several new binding partners of Pellino-2 that are localized in different intracellular compartments. In addition, we present a detailed localization study of Pellino-2 using subcellular fractionation, immunofluorescence, and live-cell imaging experiments, revealing a dynamic localization of Pellino-2 within the cell, dependent, among others, on the intracellular concentration of K^+ ions.

Materials and methods

Expression vectors

Human *PELI2* cDNA encoding full-length human Pellino-2 (UniProt ID: Q9HAT8), including a C-terminal myc and FLAG tag was subcloned from a pLenti-Peli2-myc-DDK vector (OriGene, Rockville, MD, USA, #RC203409L1) into a pQCXIH/pQCXIP expression vector (Clontech, Mountain View, CA, USA), using BamHI and EcoRI restriction enzymes. An N-terminal GFP tag was inserted containing a linker between the GFP and Pellino-2, consisting of six amino acids (Ser-Gly-Leu-Arg-Ser-Ala) [18].

HA-insulin receptor substrate-1 (IRS-1; vector ID: VB170108-1009arr) and TRAF7-HA (vector ID: VB160907-1025yut) encoding plasmids were purchased from VectorBuilder Biosciences Inc. (Guangzhou, China).

Cell culture

Primary cell culture of human fibroblasts was established as previously described [19] after informed written consent and approval of the Regional Committee for Medical and Health Research Ethics, Western Norway (IRB.no.00001872, project number 2014/59). The following immortalized cell lines normal rat kidney cells-enhanced GFP-Rab1 (NRK-eGFP-Rab1) [18], human embryonic kidney cells 293 (HEK293; ATCC, Manassas, VA, USA; #CRL-1573™), HeLa (ATCC, Manassas, VA, USA; #ATCC CCl-2™), U87MG (ATCC, Manassas, VA, USA; #ATCC HTB-14™), lymph node carcinoma of the prostate cell line (LNCaP; ATCC, Manassas, VA, USA; #ATCC CRL-1740™), and BJ-5ta immortalized fibroblasts (ATCC, Manassas, VA, USA; #ATCC CRL-4001™) were cultured under standard conditions (see Supporting information).

Yeast two-hybrid screen

The yeast two-hybrid screen was performed by Hybrigenics Services (Paris, France). Briefly, full-length human *PELI2* cDNA in an N-LexA-bait-C fusion vector was used as bait, and a human lung cancer random primed cDNA fragment library as prey. The number of analyzed interactions was 98.1 million. The positive clones were isolated and their corresponding prey fragments were Sanger-sequenced and identified using the NCBI GenBank Database. A predicted biological score was calculated for each candidate, assessing the reliability of each protein–protein interaction (highest probability of specificity: score A; lowest probability of specificity: score E).

Transient transfection, cell lysis, and co-immunoprecipitation

HEK293 cells were seeded on 10-cm plates and transient transfection was performed at 60–70% confluency. Transfection mix consisted of 8 μL Lipofectamine 2000 reagent (Invitrogen, Waltham, MA, USA, #11668019) and 2 μg plasmid DNA encoding FLAG-tagged human Pellino-2.

Cells were harvested after 40 h (see Supporting information). Due to low endogenous expression of TRAF7 and IRS-1, 2 μg of TRAF7-HA or HA-IRS-1 constructs were co-transfected with FLAG-tagged Pellino-2 for co-immunoprecipitation experiments with these proteins.

The cells were lysed in 50 mM Tris/HCl pH 7.5, 200 mM NaCl, 5 mM EDTA, 0.1% NP40, 0.5% Tween 20, 1 mM PMSF and supplemented with Complete protease inhibitors (Roche Diagnostics, Mannheim, Germany, #11-836-145-001).

For roundabout homolog 1 (ROBO-1) and HA-IRS-1 detection, the lysis buffer included additional 5% Triton X-100. Cell lysates were centrifuged to remove cell debris. The anti-immunoglobulin G (IgG) magnetic beads (New England Biolabs INC, Ipswich, MA, USA, #S1431S) and the anti-FLAG M2 magnetic beads (Sigma-Aldrich, St. Louis, MO, USA, #M8823) were washed three times with PBS, before incubation with cell supernatants for 90 min at room temperature, followed by a washing step using PBS with 0.5% Triton X-100. Bolt lithium dodecyl sulfate sample buffer (Thermo Fischer, Waltham, MA, USA, #B0007) and Bolt sample reducing agent (Thermo Fischer, Waltham, MA, USA, #B0009) were added before immunoblot analysis.

Immunoblot analysis

Proteins were separated and transferred onto nitrocellulose membranes using the Bolt® Bis-Tris Plus electrophoresis and transfer system (Thermo Fischer Scientific), as previously described [9] (see Supporting information).

Immunofluorescence

The staining procedure was performed in accordance with Sannerud *et al.* (2008) [20] and as previously described [9] (see Supporting information).

Drug treatment

HEK293 cells were treated with 10 mM tetraethylammonium chloride (TEA) before fixation for 30 min using 3% paraformaldehyde (PFA) in phosphate buffer (PB) or with 10 μM nigericin for 1 h before fixation for 30 min using 3% PFA in PBS. The staining procedure was performed as described above and in the Supporting information. TEA is a quaternary ammonium cation, comparable in size to a hydrated K^+ ion. This confers its pharmacological property as a blocker of both voltage-dependent as well as calcium-activated K^+ channels. Conversely, nigericin acts as a K^+ ionophore through an antiporter mechanism and promotes K^+ efflux.

Subcellular fractionation

HEK293 cells were homogenized in cold homogenization buffer (10 mM HEPES pH 7.4, 50 mM sucrose, 1 mM PMSF, 1 μg·mL^{-1} aprotinin, supplemented with Complete protease inhibitors Roche) using a cell homogenizer (Isobiotec, Heidelberg, Germany). The cell lysate was centrifuged at 4 °C and 2000 *g* for 10 min. The pellet (nuclear fraction) was resuspended in homogenization buffer. The supernatant (cytoplasmic fraction) was centrifuged at 100 000 *g* at 4 °C for 60 min. After resuspension in homogenization buffer and centrifugation at 100 000 *g* at 4 °C for 15 min, the pellet (membranous fraction) was resuspended

in homogenization buffer. Acetone precipitation was performed on all three fractions and resuspended in equal amount of sample buffer for immunoblot analysis (see Supporting information).

Transgenic cell preparation and culture

Transgenic BJ-5ta immortalized fibroblasts were generated by transduction with the pQCXIH/pQCXIP expression vector containing the N-terminal GFP tagged Pellino-2 construct described above [9,18]. Virus production was performed by transfecting Phoenix-AMPHO packaging cells (ATCC, Manassas, VA, USA, #CRL-3213) as described previously [21]. Two days after transfection, the medium was harvested and BJ-5ta immortalized fibroblasts (ATCC, Manassas, VA, USA, #CRL-4001) were transduced following standard protocols [22]. The cells were grown in Dulbecco's Modified Eagle Medium (DMEM) containing 10% fetal calf serum. Two days postinfection, stably transduced cells were selected by adding 10 ng·mL^{-1} puromycin (InvivoGen, San Diego, CA, USA, #ant-pr-1) to the culture medium and kept thereafter in selection medium for additional 14 days.

Live-cell imaging

Transgenic BJ-5ta immortalized fibroblasts stably overexpressing Pellino-2 with an N-terminal GFP tag were seeded in 35-mm culture dishes (no. 1.5 coverslip, 14 mm glass diameter, uncoated, MatTek, #P35G-1.5-14-C) for live-cell imaging. The Andor Dragonfly 505 confocal spinning disk system was used, under temperature and CO_2 control (37 °C and 5% CO_2), with an iXon 888 Life EMCDD camera, laser line 488 nm, 40× objective CFI Plan Apochromat Lambda S LWD and 1.14 NA. Imaging was performed over the course of 4 h, every 15 s, speed rate 20 fps.

Statistical analysis and reproducibility

Paired *t*-test was performed for band intensity quantification of ROBO-1, NEL9, disheveled homolog 2 (DVL-2), and cyclin-F co-immunoprecipitation. One-way repeated measured ANOVA, followed by Dunnett's multiple comparisons test was performed for statistical analysis of IRS-1 and TRAF7.

All results have been replicated in at least 3 independent experiments.

Results

Interaction partners of Pellino-2

Initially, we aimed at identifying novel protein–protein interactions involving Pellino-2 by employing a yeast two-hybrid screen (Table 1). The assay yielded 246 positive clones. Data analysis indicated that Pellino-2

interacts with cyclin-F, DVL-2, TNF receptor-associated factor 7 (TRAF7), and ROBO-1 with very high confidence, IRS-1, and NIMA-related kinase 9 (NEK9) with high confidence, as well as other proteins, with lower confidence interaction score (Table 1).

To validate the yeast two-hybrid data, we overexpressed FLAG-tagged Pellino-2 in HEK293 cells (Fig. 1B,D, Figs S1 and S2) and performed co-immunoprecipitation experiments to confirm these putative interaction partners of Pellino-2. Using magnetic beads coated with anti-mouse IgG, we showed that there is no unspecific binding of our proteins of interest to the beads (Fig. S1A). We also validated our experimental setup by testing known interaction partners of Pellino-2 and found that endogenous TRAF6, IRAK-1, and TAK-1 do indeed bind to overexpressed Pellino-2, while endogenous IRAK-4 did not bind in this experimental setting (Fig. S1B).

We then examined the six proteins with very high (cyclin-F, DVL-2, TRAF7 and ROBO-1) and high (IRS-1 and NEK9) confidence interaction score and confirmed that they interact with Pellino-2 also by co-immunoprecipitation (Fig. 1A,C and Fig. S1C). Due to low endogenous levels of IRS-1 and TRAF7, HA-tagged IRS-1 and TRAF7 vectors were cotransfected with Pellino-2 (Fig. 1C and Fig. S2). Quantification of band intensity for each co-immunoprecipitated protein and statistical analysis revealed significant binding of all studied proteins to FLAG-tagged Pellino-2, compared to nontransfected samples (Fig. 1E,F).

Intracellular localization of Pellino-2 and the influence of potassium

Initially, we observed that in a variety of nonimmune cell lines including cancerous, noncancerous,

Table 1. Pellino-2 candidate interacting partners identified via yeast two-hybrid screening. The binding of Pellino-2 to these proteins occurs at different locations in their structure: Pellino-2 binds to NEK9 and cyclin-F in regions that are rich in proline, serine, and threonine amino acids; DVL-2 and TRAF7 bind Pellino-2 in domains involved in their oligomerization status and therefore their activity. Binding of Pellino-2 to IRS-1 and ROBO-1 occurs on the very last amino acids at the far end C terminus of these proteins. CEP170B, Centrosomal protein 170B; DLV-2, disheveled segment polarity protein 2; MUPP1, Multi-PDZ domain protein 1; N/A, not available; NEK9, Never in mitosis A (NIMA)-related kinase 9; RBBP-8, Retinoblastoma binding protein 8; RNF220, RING finger protein 220; ROBO-1, Roundabout guidance receptor 1; TGM-2, Transglutaminase 2; TRAF7, TNF receptor-associated factor 7.

Gene name (UniProt ID)	Protein name	Intracellular localization	PBS[a]	No. positive clones/total	Binding site (aa)	Known functions in and around the binding site
CCNF (P41002)	Cyclin-F	Nucleus, centriole	A	20/246	693–762	582–766 aa: PEST-rich region
DVL2 (O14641)	DVL-2	Cytoplasm	A	13/246	141–222	11–93 aa: DIX domain, responsible for homooligomerization
						160–232 aa: DEP domain, membrane targeting of the DVL protein
						267–339 aa: PDZ domain: anchoring of signaling complexes at cellular membranes
RFWD1 (Q6Q0C0)	TRAF7	Cytoplasm	A	88/246	56–82	131–164 aa: RING-type zinc finger
						222–278 aa: TRAF-type zinc finger
ROBO1 (Q9Y6N7)	ROBO-1	Cell surface, plasma membrane	A	7/246	1243–1270	Far C-terminal part of the protein
IRS1 (P35568)	IRS-1	Plasma membrane, cytosol	B	4/246	1161–1242	Far C-terminal part of the protein
NEK9 (Q8TD19)	NEK9	Cytosol, nucleus	B	6/246	814–979	913–933 aa: coiled coil domain, responsible for dimerization
						765–888 aa: PEST-rich domain
KIAA0284 (Q9Y4F5)	CEP170B	Nucleus	C	3/246	N/A	N/A
PRR36 (Q9H6K5)	Proline rich 36	N/A	C	2/246	N/A	N/A
RBBP8 (Q99708)	RBBP-8	Nucleus	C	5/246	N/A	N/A
MPDZ (O75970)	MUPP1	Cytoplasm	D	1/246	N/A	N/A
MYO10 (Q9HD67)	Unconventional Myosin X	Cytosol	D	1/246	N/A	N/A
FLJ10597 (Q5VTB9)	RNF220	Cytoplasm	D	6/246	N/A	N/A
TGM2 (P21980)	TGM-2	Cytosol, mitochondria	E	27/246	N/A	N/A

[a]PBS, Predicted Biological Score (A = very high confidence in the interaction; B = high confidence in the interaction; C = good confidence in the interaction; D = moderate confidence or false positives; E = nonspecific interactions).

immortalized, and primary cell lines, Pellino-2 localization varied depending on the buffer used for dissolving the PFA for fixation. When 0.1 M PB pH 7.2, lacking K^+ ions, was used as fixation buffer, endogenous Pellino-2 was localized in the nucleus (Fig. 2A and

Video S1), except in HeLa cells. In contrast, when PBS pH 7.4, with physiological levels of K^+, was used as a fixation buffer, Pellino-2 was localized in the cytoplasm, in a puncta-like pattern (Fig. 2B and Video S2). PB and PBS are commonly interchangeable in
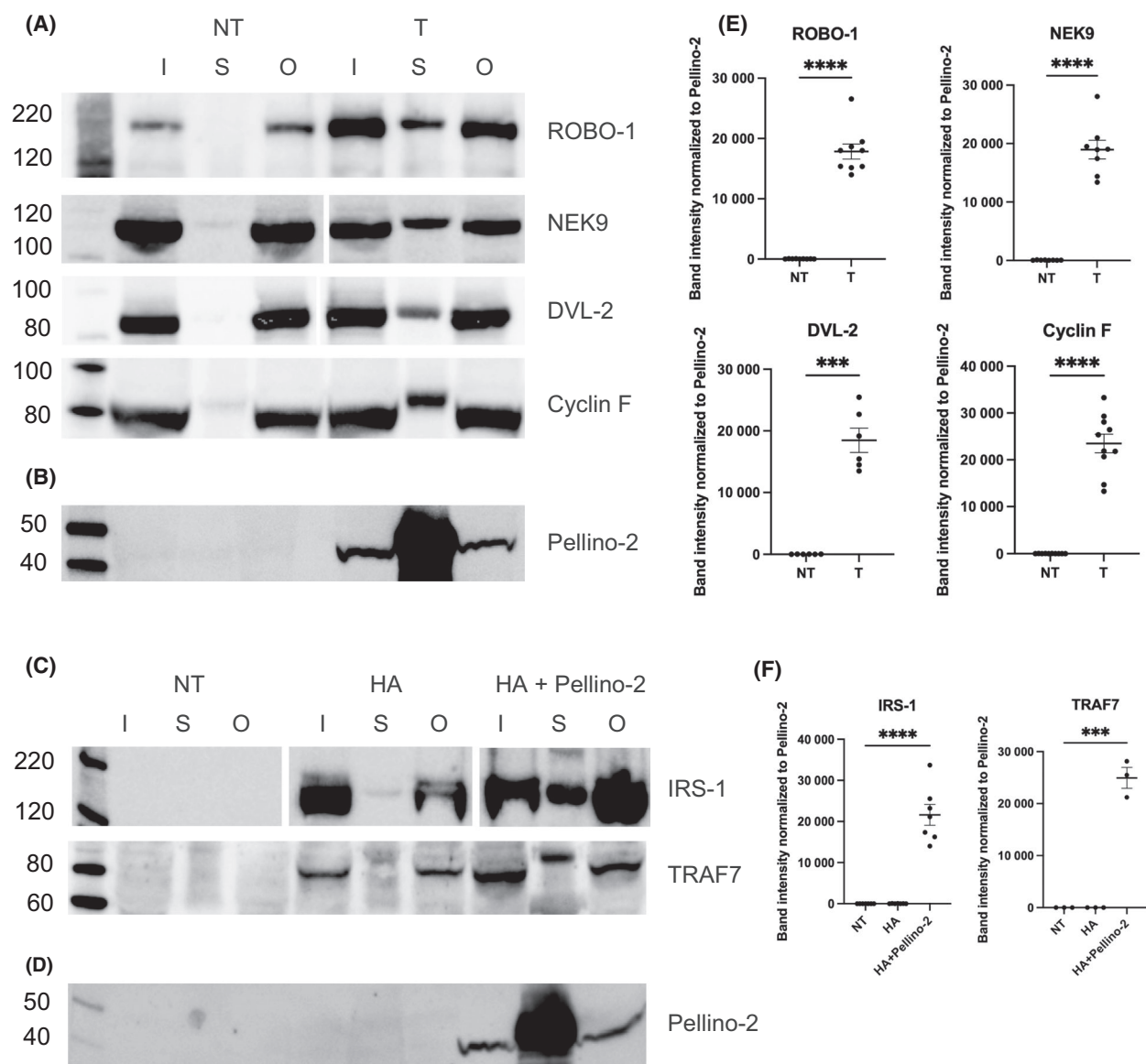

Fig. 1. Pellino-2 directly binds to putative interaction partners. HEK293 cells were transiently transfected with FLAG-tagged Pellino-2 and co-immunoprecipitated using FLAG beads (A–D). Inputs (I) at the beginning of the experiments, outputs (O) at the end of the experiments and the sample beads (S) were collected for both transfected (T) and nontransfected cells (NT). (A) Immunoblotting of putative binding partners of Pellino-2: ROBO-1, NEK9, DVL-2, and cyclin-F. (B) Immunoblotting of transfected Pellino-2, corresponding to (B). (C) Immunoblotting of putative binding partners of Pellino-2: HEK293 cells were co-transfected with Pellino-2 and HA-tagged IRS-1 and TRAF7, followed by HA detection. (D) Immunoblotting of transfected Pellino-2, corresponding to (C). (E) Statistical analysis of co-immunoprecipitated bands for nontransfected (NT) and transfected (T) samples for each novel binding partner. Data are shown as mean ± SEM of biological replicates as follows: ROBO-1 $N = 9$, NEK9 $N = 8$, DVL-2 $N = 6$, cyclin-F $N = 10$. Paired t-test was performed for band intensity quantification of ROBO-1, NEL9, DVL-2, and cyclin-F co-immunoprecipitation. (F) Statistical analysis of co-immunoprecipitated bands for nontransfected (NT) and transfected (T) samples for IRS-1 ($N = 7$) and TRAF7 ($N = 3$). Data are shown as mean ± SEM of biological replicates. One-way repeated measured ANOVA, followed by Dunnett's multiple comparisons test was performed for statistical analysis. ***$P < 0.001$, ****$P < 0.0001$.

routine immunofluorescence experiments. When we analyzed the composition of the two buffers (Table S1), we could show that Pellino-2 localization was determined by whether K^+ was present at physiological levels or not (Fig. 2, Videos S1 and S2).

When the cells were incubated with TEA prior to fixation with the PB buffer, thus blocking K^+ efflux, Pellino-2 was seen in the cytoplasm (Fig. 2C and Video S3). Additionally, we performed immunofluorescence analysis after adding various amounts of KCl to the PB fixation buffer (Fig. S3). We observed that the Pellino-2 shuttling could be attributed to the variations in the K^+ concentration of the fixation buffer.

We then incubated HEK293 cells with nigericin, to increase K^+ efflux from the cells. Even when fixation was performed with K^+-containing PBS fixation buffer, Pellino-2 changed to a nuclear localization (Fig. 2D and Video S4), further confirming that K^+ efflux affects the intracellular localization of Pellino-2.

The cytoplasmic localization of Pellino-2 under physiological conditions was further confirmed in cell fractionation experiments where Pellino-2 was found predominantly in the membranous fraction of the cytoplasm, irrespective of the K^+ content of the culture medium (Fig. 3 and Fig. S5).

Next, we investigated the localization of Pellino-2 during cell division. Pellino-2 was symmetrically localized during mitosis and was present in a punctate pattern during the late stages of division (Fig. S4).

We further examined if Pellino-2 associates with organelles in the cytoplasm. We did not observe colocalization of Pellino-2 with any of the examined protein markers: golgi matrix protein 130 (GM130), acetylated α-tubulin, translocase of outer mitochondrial membrane 20 (TOMM20), ATPase inhibitory factor 1 (ATPIF1), lysosomal-associated membrane protein 1 (LAMP-1), microtubule-associated proteins 1A/1B light chain 3 (LC3), proteasome 19S S5A/ASF, and Ras-related protein Rab1 (Fig. S6). When using PB as fixation buffer to get a nuclear localization of Pellino-2, we observed no co-localization with common nuclear markers: splicing factor SC-35, promyelocytic leukemia (PML) nuclear bodies, and proliferating cell nuclear antigen (PCNA) (Fig. S7).

Pellino-2 localization in living cultured cells

Our initial *in vitro* observations of endogenous Pellino-2 indicated that it is a dynamic protein that can change intracellular localization. To visualize Pellino-2 in living cultured cells, we proceeded to investigate it in overexpression systems.

We tested different molecular tags for Pellino-2 (Fig. S8). When HEK293 cells were transiently transfected with either FLAG-, HA- (Fig. S8A), or N-terminal or C-terminal GFP-tagged Pellino-2 (Fig. S8B), Pellino-2 was located in the cytoplasm of resting cells. In HEK293 cells overexpressing GFP-tagged Pellino-2, what appeared to be protein aggregates could be seen as a single dot in each cell (Fig. S8B).

Finally, we investigated the localization of GFP-tagged Pellino-2 in a stably transfected cell line, by performing confocal live-cell imaging (Video S5). In BJ-5ta immortalized fibroblasts overexpressing GFP-tagged Pellino-2, the protein was observed in advancing and retracting membrane protrusions (ruffles), as well as in mobile protein aggregates. Overexpressed Pellino-2 was very dynamic in nature, as it condensed in aggregates that appeared and disappeared at different locations inside the cells, as well as traveling to different parts of the cells (Video S5). The protein aggregates observed in fixed HEK293 cells (Fig. S8B) were also visible in live imaging of the transgenic BJ-5ta immortalized fibroblasts. During cell division, the GFP-tagged Pellino-2 had a similar localization as in fixed cells: The protein was found throughout the cytoplasm in interphase and symmetrically localized during mitosis (Video S5).

Discussion

In this study, we present novel binding partners of Pellino-2, localized in different intracellular compartments, and show that Pellino-2 is a dynamic protein whose localization in nonimmune cells is dependent, among others, on K^+ efflux and thus the intracellular concentration of K^+ ions.

Novel interaction partners

Using a yeast two-hybrid screen, we found 13 new potential binding partners of Pellino-2 and we confirmed the top six interactions, IRS-1, NEK9, TRAF7, cyclin-F, ROBO-1, and DVL-2, in co-immunoprecipitation experiments. Co-immunoprecipitation experiments have some pitfalls, for instance that capacity for appropriate post-translational modifications may be exceeded. Furthermore, co-immunoprecipitation requires cell lysis; therefore, cellular integrity is affected, and potential protein interactions identified may not be relevant to the intact cell. To minimize problems with overexpression and nonspecific interactions, we made several adjustments to the co-immunoprecipitation protocol. This included using reduced DNA amounts and adjustment of salt and detergent concentrations in the lysis buffer to eliminate weak interactions, as described in Materials and Methods. We were able to confirm that the binding

(A) PB fixation

(B) PBS fixation

(C) PB fixation

(D) PBS fixation

Fig. 2. Endogenous Pellino-2 changes localization depending on K$^+$ efflux. Immunofluorescence was performed in HeLa, HEK293, LNCaP, U87MG cells, and human fibroblasts to detect endogenous Pellino-2. Fixation was performed with 3% PFA in (A) 0.1 M PB pH 7.2 or (B) PBS pH 7.4. Immunofluorescence was performed in HEK293 cells, to detect endogenous Pellino-2. HEK293 cells were treated with (C) 10 mM TEA for 1 h before fixation with 3% PFA in 0.1 M PB pH 7.2 or (D) with 10 μM nigericin for 1 h before fixation with 3% PFA in PBS pH 7.4. The fluorescent images show the endogenous protein (Pellino-2) and nuclei (DAPI). Scale bar: 20 μm.
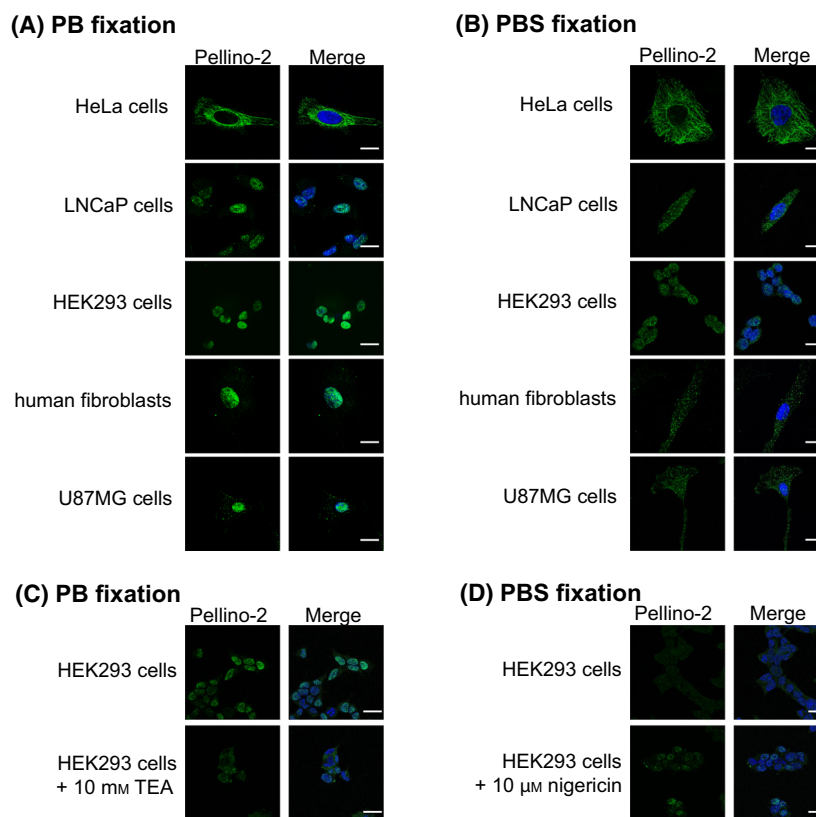
to Pellino-2 of these proteins is statistically significant compared to nontransfected samples.

ROBO-1 is a transmembrane receptor, while DVL-2, TRAF7, and IRS-1 are cytosolic proteins that elicit various functions in intracellular signaling cascades. Cyclin-F and NEK9, through different mechanisms, are key to the division of cells and localize to the nucleus and the centrosome.

The cell surface receptor ROBO-1 belongs to the family of immunoglobulin-like cell adhesion molecules and has been involved in neuronal migration and axonal guidance [23], as well as immune cell migration [24,25]. Although little is known about the ubiquitination of ROBO-1, the deubiquitinating enzyme USP33 has been shown to bind to the ROBO-1 cytoplasmic tail, protecting the receptor from proteasomal degradation [26,27]. It remains to be shown whether Pellino-2 leads to ROBO-1 ubiquitination and proteasomal targeted degradation.

DVL-2 is a central node in the Wnt/β-catenin pathway, involved in both developmental and cancerous processes. Our yeast two-hybrid data suggest that DVL-2 binds to Pellino-2 via its disheveled (DEP) domain (aa 160–232), involved in the membrane targeting of the disheveled protein [28]. Protein levels and stability of DVL-2 are regulated through the autophagy-lysosomal pathway [29,30], as well as the ubiquitin-proteasome pathway [31–33]. Furthermore, DVL-2 autophagic degradation is suppressed by interaction with IRS-1/2, which leads to Wnt-mediated cell proliferation and induction of epithelial-mesenchymal transition [34]. This has been postulated to be achieved by IRS-1/2 blocking Lys-63-linked poly-ubiquitination of DVL-2 by impairing the activity of an E3 ubiquitin ligase. We have found that Pellino-2 is a binding partner of both IRS-1 and DVL-2, and we hypothesize that Pellino-2 is the linking element between IRS-1/2 and Wnt/β-catenin signaling during EMT and cell proliferation. If DVL-2 ubiquitination is mediated by Pellino-2, then it is conceivable that IRS-1 interacts with the E3 ubiquitin ligase, deviating it from poly-ubiquitinating DVL-2. This would then lead to increased Wnt-related gene expression.

IRS-1 is a key protein in the intracellular signaling of insulin, required for the hormonal control of metabolism [35]. In our yeast two-hybrid assay, IRS-1 bound Pellino-2 at its most C-terminal amino acids (aa 1161–1242). Interestingly, IRS-1 and another member of the Pellino family, Pellino-1, have been recently implicated in a common molecular mechanism of sunitinib-induced hypertension via insulin resistance and Pellino-1 downregulation [36].
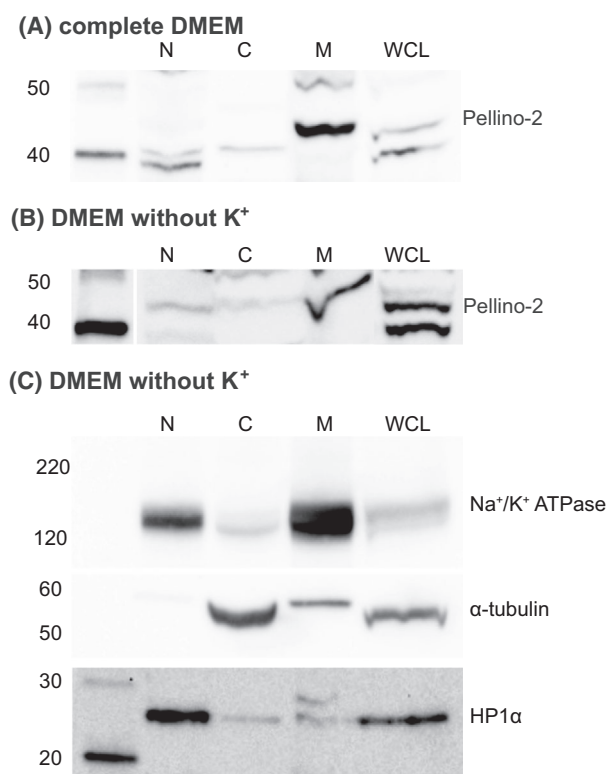
(A) complete DMEM

(B) DMEM without K⁺

(C) DMEM without K⁺

Fig. 3. Potassium ions in the cell culture medium do not affect the subcellular fractionation of Pellino-2. HEK293 cells were cultured in (A) complete DMEM culture medium or (B) custom-made DMEM culture medium lacking K⁺ ions. Subcellular fractionation of the cells and immunoblotting of Pellino-2 were performed in nuclear (N), cytoplasmic (C), and membranous (M) fractions, as well as whole cell lysate (WCL). (c) Markers for the membranous (Na⁺/K⁺-ATPase), cytoplasmic (α-tubulin), and nuclear (HP1α) fractions were also immunoblotted.

We also found that TRAF7 interacts with Pellino-2 at the N terminus of TRAF7, the binding taking place between amino acids 56–82 of TRAF7 and both possessing E3 ubiquitin ligase activity. This stretch of amino acids precedes two important domains of TRAF7 that confer catalytic activity to the protein: zinc finger domains RING-type (aa 131–164) and TRAF-type (aa 222–278). TRAF7, alongside TRAF6, has been shown to be deubiquitinated by a Lys-63-deubiquitinase, CYLD [37] and although it has been shown that TRAF7 undergoes auto-ubiquitination [38], no E3 ligases targeting TRAF7 have been reported to date. Functional studies are thus required to clarify the relationship between Pellino-2 and TRAF7. Interestingly, TRAF7 also binds to the C terminus of ROBO-4 in endothelial cells, regulating endothelial permeability in inflammation [39]. ROBO-4 is part of the roundabout family of proteins, alongside

ROBO-1, and the two receptors can form heterodimers that promote endothelial cell mobility [40,41].

The last two of the confirmed interaction partners of Pellino-2, cyclin-F and NEK9, are both involved in cell division, and both localize to the nucleus with multiple nuclear localization signals in their sequences [42,43]. We show that Pellino-2 binding to cyclin-F and NEK9 occurs at the C terminus of each of the proteins, where a peptide sequence rich in proline, glutamic acid, serine, and threonine (PEST) region is present for both of them (Table 1).

Peptide sequence rich in proline, glutamic acid, serine, and threonine sequences lead to ubiquitin-dependent degradation and result in protein instability [44]. Future functional experiments may show the involvement of Pellino-2, as an E3 ubiquitin ligase, in regulating the rapid turnover of cyclin-F.

NEK9 is a serine/threonine kinase, controlling mitosis by regulating the formation of the mitotic spindle [45]. More recently, NEK9 has been implicated in protective mechanisms against autophagy [46]. Activated, NEK9 will phosphorylate NEK6 and NEK7 and these kinases further assist with the formation and/or maintenance of the mitotic spindle [47]. To date, no mechanisms of NEK9 degradation have been described. Here, we propose Pellino-2 as a binding partner of NEK9, given their interaction at amino acids 814–979 in the NEK9 sequence. Between amino acids 765–888, NEK9 presents a PEST-rich region and between amino acids 892–939, a coiled-coil domain that leads to its dimerization. Future studies will prove if Pellino-2 mediates the ubiquitination of NEK9, thus affecting its ability to dimerize and exert its catalytic activity.

In our experimental setup, we used as positive controls previously known interaction partners of Pellino-2: IRAK-1 [10–15], IRAK-4 [13,16], TAK-1 [7,14], and TRAF6 [7,14,15]. While we confirmed that IRAK-1, TAK-1, and TRAF6 bind to Pellino-2, this was not the case for IRAK-4. Strelow et al. [13] identified Pellino-2 as an interaction partner of IRAK-4 using the latter as bait. However, upon co-transfection with Pellino-2, the binding was weak and IRAK-4 did not present any ubiquitination [13]. We therefore hypothesize that Pellino-2 binding to IRAK-4 may be mediated by common interactions partners rather than by direct binding.

While Pellino-2 has been shown to interact directly with the NLRP3 inflammasome [8,9], also several of its binding partners are known to be involved with the inflammasome: IRAK-1 [8], TAK-1 [48], NEK7 (a substrate of the novel interaction partner NEK9) [49,50], and IRS-1 [51].

Effect of potassium

We recently reported that, in THP1-derived macrophages, Pellino-2 is essential for mediating the effect of K^+ efflux on NLRP3 inflammasome activation [9]. More specifically, Pellino-2 was seen changing intracellular localization and colocalizing with NLRP3 and ASC proteins in activated THP1-derived macrophages. Pharmacological K^+ channel blockers hindered the relocation of Pellino-2 and thereby prevented assembly of the NLRP3 inflammasome [9].

In this work, we showed that Pellino-2 has a cytoplasmic localization in a wide range of nonimmune cells under physiological K^+ concentrations (Fig. 2). Interestingly, this Pellino-2 cytoplasmic localization changed upon treatment with the K^+ ionophore nigericin. As K^+ efflux was facilitated by nigericin, Pellino-2 relocated to the nucleus.

In cells fixed under nonphysiological conditions (using a K^+-free fixation buffer), Pellino-2 had nuclear localization. It is likely that a K^+-free fixation buffer leads to K^+ efflux and thus Pellino-2 relocation. By treating cells with the K^+ channel-blocking drug TEA prior to PB fixation, this relocation was no longer observed. These findings are in line with our previous studies: in immune cells, Pellino-2 changes localization due to K^+ efflux and colocalizes with NLRP3 and ASC, to facilitate inflammasome activation [9]. The functional significance of the Pellino-2 relocation due to K^+ efflux in nonimmune cells is still unclear, although it does allow Pellino-2 to access its nuclear interaction partners.

It should be noted that the response of nonimmune and immune cells to K^+ efflux seems to differ. While immune cells readily respond to cultivation in K^+-free medium [9], nonimmune cells cultured in K^+-free medium did not show a difference in Pellino-2 subcellular localization (Fig. 3). This indicates that immune cells are more sensitive to changes in extracellular K^+ and that nonimmune cells could have stronger mechanisms for maintaining homeostasis when extracellular K^+ is low. These mechanisms are a topic for further studies. However, K^+ gradients across the plasma membrane are needed for numerous processes, and the ion pump Na^+/K^+-ATPase can be fine-tuned due to its many isoforms to suit different cell types [52], while the distribution of the many types of K^+ channels varies in immune and nonimmune cells [53,54].

Dynamic Pellino-2

Given that Pellino-2 has interaction partners in various intracellular localizations and can change localization

depending among others on K^+ efflux, it seems that Pellino-2 is a dynamic protein. In static experimental setups, for example, subcellular fractionation (Fig. 3) or immunofluorescence (Fig. 2), Pellino-2 was found only in one cellular compartment at a time. However, in live-cell imaging and in experiments altering K^+ efflux across membranes, the relocation of Pellino-2 was readily visible, with Pellino-2 moving into different areas, possibly to meet its interaction partners.

Other E3 ubiquitin ligases, such as Smurf2 [55], FBXW7 [56], HERC2 [57], or MAFbx [58], have been shown to change intracellular localization upon certain stimuli. Such protein translocation between different subcellular compartments is an essential part of biological and pathological processes. While we identified K^+ efflux as a potential signal for Pellino-2 relocation, a large number of other signals such as oxidative stress [59,60], immune stimuli [61], neddylation [62], hypoxia [63], endoplasmic reticulum stress [64], phosphorylation [65], or fasting [66] are also recognized signals that can lead to dynamic redistribution of proteins inside cells.

In conclusion, our work suggests that the E3 ubiquitin ligase Pellino-2 is a dynamic protein, that can change intracellular localization following K^+ efflux, and that may be involved in a variety of intracellular signaling pathways, such as cell migration via ROBO-1, epithelial–mesenchymal transition via DVL-2, insulin signaling via IRS-1, or cell division via cyclin-F and NEK9.

Acknowledgements

Author contributions

OB, ER, and CB conceived and supervised the study. IC and OB conducted the experiments. IC, ER, and

CB wrote the manuscript. IC, OB, IA, ER, and CB analyzed the results and reviewed the manuscript.

Data accessibility

The data that support the findings of this study are available in the supplementary material of this article.

References

1 Grosshans J, Schnorrer F and Nusslein-Volhard C (1999) Oligomerisation of tube and pelle leads to nuclear localisation of dorsal. *Mech Dev* **81**, 127–138.

2 Moynagh PN (2014) The roles of Pellino E3 ubiquitin ligases in immunity. *Nat Rev Immunol* **14**, 122–131.

3 Medvedev AE, Murphy M, Zhou H and Li X (2015) E3 ubiquitin ligases Pellinos as regulators of pattern recognition receptor signaling and immune responses. *Immunol Rev* **266**, 109–122.

4 Chang M, Jin W and Sun SC (2009) Peli1 facilitates TRIF-dependent Toll-like receptor signaling and proinflammatory cytokine production. *Nat Immunol* **10**, 1089–1095.

5 Siednienko J, Jackson R, Mellett M, Delagic N, Yang S, Wang B, Tang LS, Callanan JJ, Mahon BP and Moynagh PN (2012) Pellino3 targets the IRF7 pathway and facilitates autoregulation of TLR3- and viral-induced expression of type I interferons. *Nat Immunol* **13**, 1055–1062.

6 Yang S, Wang B, Humphries F, Hogan AE, O'Shea D and Moynagh PN (2014) The E3 ubiquitin ligase Pellino3 protects against obesity-induced inflammation and insulin resistance. *Immunity* **41**, 973–987.

7 Jensen LE and Whitehead AS (2003) Pellino2 activates the mitogen activated protein kinase pathway. *FEBS Lett* **545**, 199–202.

8 Humphries F, Bergin R, Jackson R, Delagic N, Wang B, Yang S, Dubois AV, Ingram RJ and Moynagh PN (2018) The E3 ubiquitin ligase Pellino2 mediates priming of the NLRP3 inflammasome. *Nat Commun* **9**, 1560.

9 Cristea I, Bruland O, Rødahl E and Bredrup C (2021) K+ regulates relocation of Pellino-2 to the site of NLRP3 inflammasome activation in macrophages. *FEBS Lett* **595**, 2437–2446.

10 Lin CC, Huoh YS, Schmitz KR, Jensen LE and Ferguson KM (2008) Pellino proteins contain a cryptic FHA domain that mediates interaction with phosphorylated IRAK1. *Structure* **16**, 1806–1816.

11 Schauvliege R, Janssens S and Beyaert R (2006) Pellino proteins are more than scaffold proteins in TLR/IL-1R signalling: a role as novel RING E3-ubiquitin-ligases. *FEBS Lett* **580**, 4697–4702.

12 Yu KY, Kwon HJ, Norman DAM, Vig E, Goebl MG and Harrington MA (2002) Cutting edge: mouse pellino-2 modulates IL-1 and lipopolysaccharide signaling. *J Immunol* **169**, 4075–4078.

13 Strelow A, Kollewe C and Wesche H (2003) Characterization of Pellino2, a substrate of IRAK1 and IRAK4. *FEBS Lett* **547**, 157–161.

14 Kim TW, Yu M, Zhou H, Cui W, Wang J, DiCorleto P, Fox P, Xiao H and Li X (2012) Pellino 2 is critical for Toll-like receptor/interleukin-1 receptor (TLR/IL-1R)-mediated post-transcriptional control. *J Biol Chem* **287**, 25686–25695.

15 Huoh YS and Ferguson KM (2014) The pellino e3 ubiquitin ligases recognize specific phosphothreonine motifs and have distinct substrate specificities. *Biochemistry* **53**, 4946–4955.

16 Butler MP, Hanly JA and Moynagh PN (2007) Kinase-active interleukin-1 receptor-associated kinases promote polyubiquitination and degradation of the Pellino family: direct evidence for PELLINO proteins being ubiquitin-protein isopeptide ligases. *J Biol Chem* **282**, 29729–29737.

17 Muñoz-Planillo R, Kuffa P, Martínez-Colón G, Smith BL, Rajendiran TM and Núñez G (2013) K+ efflux is the common trigger of NLRP3 inflammasome activation by bacterial toxins and particulate matter. *Immunity* **38**, 1142–1153.

18 Sannerud R, Marie M, Nizak C, Dale HA, Pernet-Gallay K, Perez F, Goud B and Saraste J (2006) Rab1 defines a novel pathway connecting the pre-Golgi intermediate compartment with the cell periphery. *Mol Biol Cell* **17**, 1514–1526.

19 Bredrup C, Stokowy T, McGaughran J, Lee S, Sapkota D, Cristea I, Xu L, Tveit KS, Høvding G, Steen VM *et al.* (2019) A tyrosine kinase-activating variant Asn666Ser in PDGFRB causes a progeria-like condition in the severe end of Penttinen syndrome. *Eur J Hum Genet* **27**, 574–581.

20 Sannerud R, Marie M, Hansen BB and Saraste J (2008) Use of polarized PC12 cells to monitor protein localization in the early biosynthetic pathway. *Methods Mol Biol (Clifton, NJ)* **457**, 253–265.

21 Pear WS, Nolan GP, Scott ML and Baltimore D (1993) Production of high-titer helper-free retroviruses by transient transfection. *Proc Natl Acad Sci USA* **90**, 8392–8396.

22 Swift S, Lorens J, Achacoso P and Nolan GP (2001) Rapid production of retroviruses for efficient gene delivery to mammalian cells using 293T cell-based systems. *Curr Protoc Immunol* **Chapter 10**, Unit 10 7C.

23 Kidd T, Brose K, Mitchell KJ, Fetter RD, Tessier-Lavigne M, Goodman CS, Goodman CS and Tear G (1998) Roundabout controls axon crossing of the CNS midline and defines a novel subfamily of evolutionarily conserved guidance receptors. *Cell* **92**, 205–215.

24 Wu JY, Feng L, Park HT, Havlioglu N, Wen L, Tang H, Bacon KB, Jiang Z-H, Zhang X-C and Rao Y

(2001) The neuronal repellent Slit inhibits leukocyte chemotaxis induced by chemotactic factors. *Nature* **410**, 948–952.

25 Ye BQ, Geng ZH, Ma L and Geng JG (1950) Slit2 regulates attractive eosinophil and repulsive neutrophil chemotaxis through differential srGAP1 expression during lung inflammation. *J Immunol (Baltimore, MD: 1950)* **185**, 6294–6305.

26 Yuasa-Kawada J, Kinoshita-Kawada M, Wu G, Rao Y and Wu JY (2009) Midline crossing and Slit responsiveness of commissural axons require USP33. *Nat Neurosci* **12**, 1087–1089.

27 Jia M, Guo Y and Lu X (2018) USP33 is a biomarker of disease recurrence in papillary thyroid carcinoma. *Cell Physiol Biochem* **45**, 2044–2053.

28 Tauriello DV, Jordens I, Kirchner K, Slootstra JW, Kruitwagen T, Bouwman BA, Noutsou M, Rüdiger SGD, Schwamborn K, Schambony A et al. (2012) Wnt/ β-catenin signaling requires interaction of the dishevelled DEP domain and C terminus with a discontinuous motif in Frizzled. *Proc Natl Acad Sci USA* **109**, E812–E820.

29 Gao C, Cao W, Bao L, Zuo W, Xie G, Cai T, Fu W, Zhang J, Wu W, Zhang X et al. (2010) Autophagy negatively regulates Wnt signalling by promoting Dishevelled degradation. *Nat Cell Biol* **12**, 781–790.

30 Zhang Y, Wang F, Han L, Wu Y, Li S, Yang X, Wang Y, Ren F, Zhai Y, Wang D et al. (2011) GABARAPL1 negatively regulates Wnt/beta-catenin signaling by mediating Dvl2 degradation through the autophagy pathway. *Cell Physiol Bioch* **27**, 503–512.

31 Sharma J, Mulherkar S, Mukherjee D and Jana NR (2012) Malin regulates Wnt signaling pathway through degradation of dishevelled2. *J Biol Chem* **287**, 6830–6839.

32 Ding Y, Zhang Y, Xu C, Tao QH and Chen YG (2013) HECT domain-containing E3 ubiquitin ligase NEDD4L negatively regulates Wnt signaling by targeting dishevelled for proteasomal degradation. *J Biol Chem* **288**, 8289–8298.

33 Wei W, Li M, Wang J, Nie F and Li L (2012) The E3 ubiquitin ligase ITCH negatively regulates canonical Wnt signaling by targeting dishevelled protein. *Mol Cell Biol* **32**, 3903–3912.

34 Geng Y, Ju Y, Ren F, Qiu Y, Tomita Y, Tomoeda M, Kishida M, Wang Y, Jin L, Su F et al. (2014) Insulin receptor substrate 1/2 (IRS1/2) regulates Wnt/beta-catenin signaling through blocking autophagic degradation of dishevelled2. *J Biol Chem* **289**, 11230–11241.

35 Guo S (2014) Insulin signaling, resistance, and the metabolic syndrome: insights from mouse models into disease mechanisms. *J Endocrinol* **220**, T1–t23.

36 Liu Y, Tang LL, Liang C, Wu MM and Zhang ZR (2021) Insulin resistance and pellino-1 mediated

decrease in the activities of vasodilator signaling contributes to sunitinib-induced hypertension. *Front Pharmacol* **12**, 617165.

37 Yoshida H, Jono H, Kai H and Li J-D (2005) The tumor suppressor cylindromatosis (CYLD) acts as a negative regulator for toll-like receptor 2 signaling via negative cross-talk with TRAF6 and TRAF7. *J Biol Chem* **280**, 41111–41121.

38 Bouwmeester T, Bauch A, Ruffner H, Angrand PO, Bergamini G, Croughton K, Cruciat C, Eberhard D, Gagneur J, Ghidelli S et al. (2004) A physical and functional map of the human TNF-alpha/NF-kappa B signal transduction pathway. *Nat Cell Biol* **6**, 97–105.

39 Shirakura K, Ishiba R, Kashio T, Funatsu R, Tanaka T, Fukada SI, Tanaka T, Fukada S-I, Ishimoto K, Hino N et al. (2019) The Robo4-TRAF7 complex suppresses endothelial hyperpermeability in inflammation. *J Cell Sci* **132**, 220–228.

40 Hivert B, Liu Z, Chuang CY, Doherty P and Sundaresan V (2002) Robo1 and Robo2 are homophilic binding molecules that promote axonal growth. *Mol Cell Neurosci* **21**, 534–545.

41 Sheldon H, Andre M, Legg JA, Heal P, Herbert JM, Sainson R, Sharma AS, Kitajewski JC, Heath VL, Bicknell R et al. (2009) Active involvement of Robo1 and Robo4 in filopodia formation and endothelial cell motility mediated via WASP and other actin nucleation-promoting factors. *FASEB J* **23**, 513–522.

42 Tan BC-M and Lee S-C (2004) Nek9, a novel FACT-associated protein, modulates interphase progression. _J Biol Chem_ **279**, 9321–9330.

43 Kong M, Barnes EA, Ollendorff V and Donoghue DJ (2000) Cyclin F regulates the nuclear localization of cyclin B1 through a cyclin-cyclin interaction. *EMBO J* **19**, 1378–1388.

44 Rogers S, Wells R and Rechsteiner M (1986) Amino acid sequences common to rapidly degraded proteins: the PEST hypothesis. *Science* **234**, 364–368.

45 Fry AM, O'Regan L, Sabir SR and Bayliss R (2012) Cell cycle regulation by the NEK family of protein kinases. *J Cell Sci* **125** (Pt 19), 4423–4433.

46 Shrestha BK, Skytte Rasmussen M, Abudu YP, Bruun JA, Larsen KB, Alemu EA, Sjøttem E, Lamark T and Johansen T (2020) NIMA-related kinase 9-mediated phosphorylation of the microtubule-associated LC3B protein at Thr-50 suppresses selective autophagy of p62/sequestosome 1. *J Biol Chem* **295**, 1240–1260.

47 Bertran MT, Sdelci S, Regué L, Avruch J, Caelles C and Roig J (2011) Nek9 is a Plk1-activated kinase that controls early centrosome separation through Nek6/7 and Eg5. *Embo j* **30**, 2634–2647.

48 Malireddi RKS, Gurung P, Mavuluri J, Dasari TK, Klco JM, Chi H, and Kanneganti T-D (2018) TAK1 restricts spontaneous NLRP3 activation and cell death

to control myeloid proliferation. *J Exp Med* **215**, 1023–1034.

49 Schmid-Burgk JL, Chauhan D, Schmidt T, Ebert TS, Reinhardt J, Endl E, and Hornung V (2016) A genome-wide CRISPR (clustered regularly interspaced short palindromic repeats) screen identifies NEK7 as an essential component of NLRP3 inflammasome activation. *J Biol Chem* **291**, 103–109.

50 He Y, Zeng MY, Yang D, Motro B and Nunez G (2016) NEK7 is an essential mediator of NLRP3 activation downstream of potassium efflux. *Nature* **530**, 354–357.

51 Cho KA and Kang PB (2015) PLIN2 inhibits insulin-induced glucose uptake in myoblasts through the activation of the NLRP3 inflammasome. *Int J Mol Med* **36**, 839–844.

52 Clausen MV, Hilbers F and Poulsen H (2017) The structure and function of the Na, K-ATPase isoforms in health and disease. *Front Physiol* **8**, 1–16.

53 Colden-Stanfield M (2010) Adhesion-dependent modulation of macrophage K+ channels. *Adv Exp Med Biol* **674**, 81–94.

54 Varghese A, Tenbroek EM, Coles J Jr and Sigg DC (2006) Endogenous channels in HEK cells and potential roles in HCN ionic current measurements. *Prog Biophys Mol Biol* **90**, 26–37.

55 Di Guglielmo GM, Le Roy C, Goodfellow AF and Wrana JL (2003) Distinct endocytic pathways regulate TGF-β receptor signalling and turnover. *Nat Cell Biol* **5**, 410–421.

56 Song Y, Lai L, Chong Z, He J, Zhang Y, Xue Y, Xie Y, Chen S, Dong P, Chen L *et al.* (2017) E3 ligase FBXW7 is critical for RIG-I stabilization during antiviral responses. *Nat Commun* **8**, 14654.

57 Wu W, Sato K, Koike A, Nishikawa H, Koizumi H, Venkitaraman AR, and Ohta T (2010) HERC2 Is an E3 ligase that targets BRCA1 for degradation. *Can Res* **70**, 6384–6392.

58 Julie L-C, Sabrina B-P, Marie-Pierre L and Leibovitch SA (2012) Identification of essential sequences for cellular localization in the muscle-specific ubiquitin E3 ligase MAFbx/Atrogin 1. *FEBS Lett* **586**, 362–367.

59 Shukla S and Mishra R (2018) Level of hydrogen peroxide affects expression and sub-cellular localization of Pax6. *Mol Biol Rep* **45**, 533–540.

60 Baqader NO, Radulovic M, Crawford M, Stoeber K and Godovac-Zimmermann J (2014) Nuclear cytoplasmic trafficking of proteins is a major response of human fibroblasts to oxidative stress. *J Proteome Res* **13**, 4398–4423.

61 Mulero MC, Huxford T and Ghosh G (2019) NF-κB, IκB, and IKK: integral components of immune system signaling. *Adv Exp Med Biol* **1172**, 207–226.

62 Li S, Fang W, Cui Y, Shi H, Chen J, Li L, Zhang L and Zhang X (2020) Neddylation promotes protein translocation between the cytoplasm and nucleus. *Biochem Biophys Res Comm* **529**, 991–997.

63 Depping R, Jelkmann W and Kosyna FK (2015) Nuclear-cytoplasmatic shuttling of proteins in control of cellular oxygen sensing. *J Mol Med* **93**, 599–608.

64 Haze K, Yoshida H, Yanagi H, Yura T and Mori K (1999) Mammalian transcription factor ATF6 is synthesized as a transmembrane protein and activated by proteolysis in response to endoplasmic reticulum stress. *Mol Biol Cell* **10**, 3787–3799.

65 Lopez JP, Turner JR and Philipson LH (2010) Glucose-induced ERM protein activation and translocation regulates insulin secretion. *Am J Physiol Endocrinol Metab* **299**, E772–E785.

66 Wang T, Cao Y, Zheng Q, Tu J, Zhou W, He J, Zhong J, Chen Y, Wang J, Cai R *et al.* (2019) SENP1-Sirt3 signaling controls mitochondrial protein acetylation and metabolism. *Mol Cell* **75**, 823–34.e5.

Supporting information

Additional supporting information may be found online in the Supporting Information section at the end of the article.

Fig. S1. (A) Immunoblotting of known and potential interaction partners of Pellino-2 following co-immuno-precipitation with non-specific mouse IgG magnetic beads; (B) Immunoblotting of known interaction partners of Pellino-2: IRAK-1, TAK-1, TRAF6 and IRAK-4; (C) Complete blots corresponding to Figure 1A,B.

Fig. S2. (A) Complete blots corresponding to Figure 1C; (B) Complete blot corresponding to Figure 1D.

Fig. S3. Gradual decreases in extracellular K^+ leads to nuclear relocation of Pellino-2.

Fig. S4. Pellino-2 distribution during cell division.

Fig. S5. (A) Complete blots corresponding to Figure 3A,B; (B) Complete blots corresponding to Figure 3C.

Fig. S6. Pellino-2 immunostaining with cytosolic markers, using PBS as fixation buffer.

Fig. S7. Pellino-2 and various nuclear markers, using 0.1 M PB as fixation buffer.

Fig. S8. Intracellular localization of overexpressed Pellino-2.

Table S1. Chemical composition of buffers used for fixation.

Video S1. Pellino-2 immunofluorescence detection in HEK293 cells, fixed using fixation buffer lacking K^+ ions.

Video S2. Pellino-2 immunofluorescence detection in HEK293 cells, fixed using fixation buffer with physiological concentration of K^+ ions.

Video S3. Pellino-2 immunofluorescence detection in HEK293 cells, treated with K^+ channel blocker TEA prior to fixation using fixation buffer lacking K^+ ions.

Video S4. Pellino-2 immunofluorescence detection in HEK293 cells, treated with K^+ ionophore nigericin prior to fixation using fixation buffer with physiological concentration of K^+ ions.

Video S5. Confocal live cell imaging of stably transfected GFP-tagged Pellino-2 in immortalized fibroblasts.